

Pathways for Single-Shot All-Optical Switching of Magnetization in Ferrimagnets

C.S. Davies^{1,2,*}, T. Janssen,^{1,2} J.H. Mentink,² A. Tsukamoto,³ A.V. Kimel,²
A.F.G. van der Meer,^{1,2} A. Stupakiewicz,⁴ and A. Kirilyuk^{1,2,†}

¹*FELIX Laboratory, Radboud University, 7c Toernooiveld, 6525 ED Nijmegen, Netherlands*

²*Institute for Molecules and Materials, Radboud University, 135 Heyendaalseweg, 6525 AJ Nijmegen, Netherlands*

³*College of Science and Technology, Nihon University, 7-24-1 Funabashi, Chiba 274-8501, Japan*

⁴*Faculty of Physics, University of Białystok, 1L Ciolkowskiego, 15-245 Białystok, Poland*



(Received 5 May 2019; revised manuscript received 15 January 2020; accepted 31 January 2020; published 24 February 2020)

Single-shot helicity-independent all-optical switching of magnetization in ferrimagnets represents the fastest known approach for deterministic data recording. Recently, it was shown that 15-ps-long optical pulses could suffice in triggering the magnetic switching in certain Gd-Fe-Co alloys, generating enormous controversy about the underlying mechanism. Here, we demonstrate how the exact composition of the ferrimagnet affects the kinetics of the reversal process and facilitates the use of thermal pulses with a duration spanning all relevant timescales within the nonadiabatic limit. By modelling a generic ferrimagnet as two coupled macrospins, we show that the magnetization reversal can occur via distinctly different pathways, depending on the duration of the heater. We experimentally reveal that pulses with a duration below and above a critical pulse width respectively enable and disable the capability of all-optical magnetization switching in Gd-Fe-Co alloys, and that modest change of the alloy composition leads to drastic variation of the critical pulse width, by almost 2 orders of magnitude. Our interpretation and results resolve an urgent and outstanding technologically relevant controversy, and provide crucial but previously overlooked guidelines for how to engineer deterministic all-optical switching of magnetization in suitable ferrimagnets.

DOI: 10.1103/PhysRevApplied.13.024064

I. INTRODUCTION

The societal hunger for smaller, faster, and more energy-efficient hard-disk-drive technology stimulates intense exploration of magnetization switching processes. Historically, the industrially favored approach employs just a writing magnetic field, but fundamental geometrical and material restrictions practically prohibit strengthening of the writing field [1] beyond approximately 1 T. Instead, the two leading candidates for next-generation technologies use microwave fields [2] or light [3] to temporarily reduce the magnetic field needed to write a bit. Both microwave-assisted and heat-assisted magnetic recordings are projected [4–6] to be capable of writing information on high-density magnetic media (with storage densities surpassing 4 Tb/in² [2]) albeit on a timescale of at least 100 ps, during which the magnetization is persistently in equilibrium. It remains an open and critically important question as to how one can further increase data writing speeds.

In 1996, the pivotal discovery that demagnetization could be achieved on a subpicosecond timescale [7] gave birth to the research field of ultrafast magnetism [8,9], devoted to understanding nonequilibrium magnetic phenomena. Just over a decade later, a counterintuitive and potentially disruptive light-based approach for magnetic recording was unveiled [10], eliminating entirely the need for a magnetic field while driving writing times towards the picosecond timescale [11,12]. The umbrella process of all-optical switching (AOS), in which ultrashort optical pulses reverse magnetization, can now be achieved in a wide range of ferromagnets or ferrimagnets [13–15] using single or multiple optical pulses of different polarizations. However, to date, the only materials that have displayed ultrafast single-shot helicity-independent AOS are ferrimagnetic alloys of Gd-Fe-Co [13] and multilayered stacks of Pt/Gd/Co [16] and Tb/Co [17] (synthetic ferrimagnets). In these materials, a single optical pulse will toggle the magnetization deterministically, i.e., irrespective of the ferrimagnet's initial magnetic polarity or the optical pulse's polarization.

The process of single-shot helicity-independent AOS in Gd-Fe-Co was discovered by Radu *et al.* [18] to follow a very peculiar pathway. Upon exposure to a 60-fs optical

*c.davies@science.ru.nl

†a.kirilyuk@science.ru.nl

pulse, the magnetization of the Gd and Fe-Co sublattices decouple and demagnetize at drastically different rates [19], at a ratio of approximately 1:4. Upon crossing zero, the magnetization of the Fe-Co sublattice recovers parallel in direction to the still-demagnetizing Gd sublattice, generating a transient ferromagneticlike state. The latter is in complete opposition to the antiferromagnetic exchange coupling that exists between Gd and Fe-Co. Subsequent predominantly numerical investigations [13,20] have systematically distilled the process of AOS as stemming from two rules: if (i) the multisublattice magnet contains two substantially different sublattices that are coupled via the antiferromagnetic exchange interaction, and (ii) this ferrimagnet is excited by a laser pulse with a duration shorter than the timescale of the electron-lattice interaction τ_{e-l} [approximately 2 ps in Gd-Fe-Co], single-shot helicity-independent AOS can be achieved. The observable formation of the nonequilibrium transient ferromagneticlike state represents a crucial evolutionary prerequisite that must be met in order for deterministic AOS to proceed, since there is no other symmetry-breaking effect that can conceivably account for the toggle character of the switching process.

Enormous controversy was therefore ignited by experimental reports demonstrating that pulses longer than τ_{e-l} (even up to lengths of 15 ps) could, in certain cases, achieve single-shot helicity-independent AOS in Gd-Fe-Co [21,22]. This surprising result, falsifying the long-held assumption that deterministic AOS required rapid heating within approximately 2 ps, even led to claims [22] about the insolvency of the mechanism via a strong nonequilibrium state in general. While it is clear that a femtosecond short laser pulse generates a strong nonequilibrium state in Gd-Fe-Co [13,18–20], it is also clear that laser pulses with duration τ longer than τ_{e-l} cannot induce dramatic overheating of the free electrons [22]. Such overheating is seemingly crucial for ultrafast demagnetization as the spin-lattice relaxation rate is proportional to the effective electron temperature [23,24]. Despite the fact that the influence of the pulse duration on the process of single-shot AOS has been discussed in several articles [21,22,25], contemporary atomistic [13] and phenomenological [20] models of AOS have not yet predicted or explained how AOS can be achieved by such long pulses, leaving open a critical gap in the research field of ultrafast magnetism. Developing understanding of this process will have profound implications for technological implementations of single-shot helicity-independent AOS, since, e.g., existing semiconductor lasers are already capable of generating 10-ps-long optical pulses [26].

In this article, we resolve the controversy of how single-shot helicity-independent AOS can be achieved in a generic ferrimagnet of composition $A_{100-x}B_x$ using laser pulses with durations covering all relevant timescales. We conceptually show that two distinct pathways allow for deterministic AOS, with angular momentum flowing

either from both sublattices to the external environment, or between A and B themselves (so-called exchange relaxation). The direction of the angular momentum flow is dictated solely by the temporal duration of the excitation and the relaxation properties of the ferrimagnet. We reveal that the overarching criterion for deterministic AOS lies in the condition that the heating induces a strongly nonequilibrium state between the lattice and the two magnetic sublattices. The strength of the nonequilibrium state derives either from a sharp spike in the electronic temperature relative to the two magnetic sublattices, or from a persistent nonequilibrium that exists between the two sublattices themselves. In the latter case, even relatively slow heating of the system triggering purely exchange-driven dynamics can achieve reversal, provided that (i) there is more absolute angular momentum in B rather than in A , and (ii) the spin-lattice thermalization time is slower than the timescale of the intersublattice exchange relaxation. This pathway is underpinned by the intersublattice exchange interaction, which permits fast change of the magnetization of one of the sublattices at the cost of the other, and does not require a spike in the electronic temperature.

To validate our conceptual understanding, we use a phenomenological mean field theory describing the sublattice-resolved longitudinal magnetization dynamics of $A_{100-x}B_x$, taking into account both the temporal profile of a thermal load and the alloy composition. In spite of many simplifying assumptions, our theory successfully reproduces the key features of our posited interpretation when applied to the case of $Gd_x(FeCo)_{100-x}$ alloys. For ultimate proof, we experimentally study the material and optical parameters that enable or disable single-shot helicity-independent AOS in $Gd_x(FeCo)_{100-x}$ alloys. Specifically, we identify a critical pulse-duration threshold τ_c that defines the deterministic character of the AOS process exhibited by $Gd_x(FeCo)_{100-x}$ alloys, and increases drastically (by almost 2 orders of magnitude) with the concentration x of gadolinium. We also show that photons in a very wide spectral range, from visible to midinfrared, are equally capable of triggering deterministic AOS. Our conceptual interpretation explains both our measurements and a wealth of other experimental and numerical findings pertaining to single-shot helicity-dependent AOS in ferrimagnets that have, until now, not been unified within a common framework of understanding. Moreover, we believe our understanding may be expanded to experimentally predict the general conditions that will enable deterministic AOS in different ferrimagnetic materials, such as synthetic ferrimagnets [27].

II. CONCEPTUAL MODEL

We consider here a generic ferrimagnet AB , where sublattices A and B are ferromagnetic and paramagnetic respectively in isolation at the starting temperature of

the experiment, i.e., there is a substantial mismatch in the intrasublattice exchange-coupling constants and Curie temperatures of A and B in isolation. The intersublattice exchange coupling between the two sublattices gives rise to a common Curie temperature of AB in equilibrium, and also the existence of two degenerate equilibrium states, with A and B having antiparallel magnetization. These two states are indicated by green dots in the sublattice-resolved phase diagram of angular momentum S shown in Fig. 1, and trajectories connecting the two correspond to deterministic pathways for single-shot AOS. Under equilibrium conditions, it is impossible for AOS to occur without an assistive magnetic field. Adiabatic heating of the ferrimagnet, i.e., $\tau > \tau_{s-l}$ where τ_{s-l} is the spin-lattice thermalization time, results in S_B decreasing more rapidly than S_A (inset [28] of Fig. 1), and ends with the complete destruction of magnetization in both sublattices simultaneously. This scenario corresponds to the dashed trajectory shown in Fig. 1.

When the ferrimagnet is instead heated under nonequilibrium conditions [29], it is possible for the magnetization

of one sublattice to cross zero before the other. This transient ferromagneticlike state, observed experimentally [18] and numerically [13], represents an observable evolutionary signature of single-shot AOS, whereby switching is only achieved if the magnetization of sublattice A crosses zero before B . If instead the magnetization of B crosses zero before A , deterministic AOS fails [30]. On this basis, we therefore impose a master-slave relationship between the two sublattices, whereby the demagnetization rate of the master sublattice A (the sublattice with the much higher Curie temperature in isolation [11,31]) dictates the success of deterministic AOS.

Depending on the duration of the nonequilibrium heating, the magnetization may relax via two distinct mechanisms. The first involves intersublattice exchange coupling (with a characteristic timescale τ_{A-B}) in which the angular momentum of the master sublattice grows at the expense of the slave's. If the dynamics are driven purely by this exchange coupling, the total angular momentum of AB is conserved and so $\partial_t S_A = -\partial_t S_B$. As one therefore reduces τ from above to below τ_{s-l} , the dashed trajectory shown in Fig. 1 becomes increasingly linear along the figure diagonal (solid curve in Fig. 1). Provided that (i) there is more absolute angular momentum in slave B than in master A , and (ii) $\tau_{A-B} < \tau_{s-l}$, relatively slow heating of the system (> 10 ps) can still generate the observable signature of single-shot AOS (S_A crosses zero while S_B is demagnetizing). During this period, the master sublattice continues to receive angular momentum from the slave, until the latter's magnetization crosses zero. The duration of this transient ferromagnetic state is dictated by the relative demagnetization rates of A and B . Subsequently, the slave sublattice switches its magnetization polarity, as dictated by master A , and so deterministic AOS is successfully achieved.

Upon further reduction of τ towards the timescale of electron-lattice thermalization (approximately 2 ps in Gd-Fe-Co) [21,32], temperature-induced dissipation of S_A and S_B to the external environment overwhelms the exchange coupling, and the sublattices essentially relax independently. Furthermore, if A has a smaller spin moment than B , A will demagnetize faster [18], resulting in a reasonably horizontal dotted trajectory as indicated in Fig. 1 [in Gd-Fe-Co, this gradient is approximately 4:−1]. S_B is now even larger when S_A crosses zero, and so the already-cooling system enables the intersublattice exchange coupling and subsequent magnetization recovery to complete the switching process.

By varying the alloy concentration of $A_{100-x}B_x$, the initial and final equilibrium states (green dots in Fig. 1) will shift. Increasing x shifts the initial and final equilibrium states of AB up and down respectively in Fig. 1, allowing a steeper trajectory to join the two states. Physically, the slave has more angular momentum available to transfer to the master, allowing a longer pulse (still satisfying the nonadiabatic condition $\tau_{A-B} < \tau_{s-l}$) to achieve

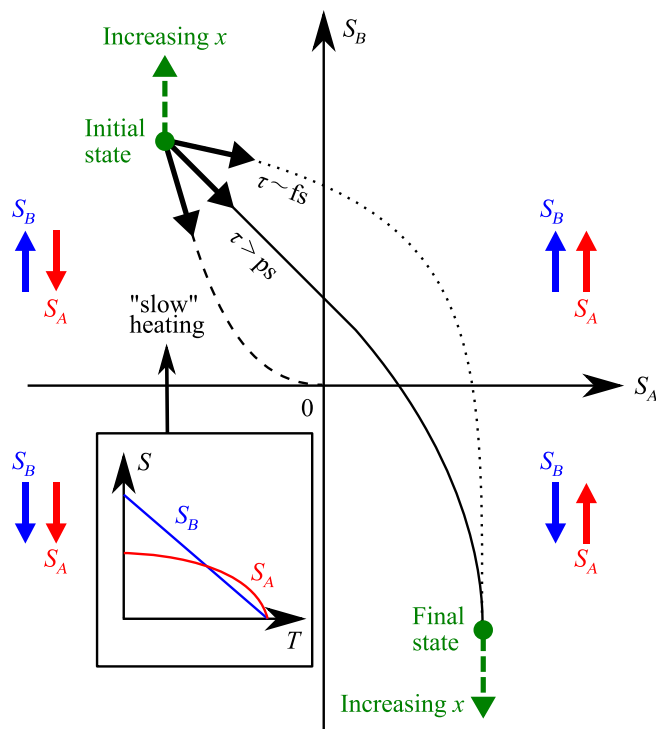


FIG. 1. Conceptual phase map showing the different pathways for thermally induced relaxation and recovery of the constituent-resolved angular momentum S of the ferrimagnet $A_{100-x}B_x$. The thick green dots indicate positions of equilibrium, and by varying x , these states are translated across the map. Excitation of the ferrimagnet by thermal pulses of varying duration τ lead to different trajectories. Shown in the inset is the adiabatic thermal dependence of the angular momentum.

deterministic AOS. Conversely, reducing x will disable the possibility for deterministic AOS to proceed via exchange coupling only, if $|S_B| < |S_A|$. However, a shorter pulse generating a more horizontal trajectory in Fig. 1 would still suffice.

III. NUMERICAL MODELLING

To numerically test our conceptual understanding summarized in Fig. 1, we expand upon the phenomenological mean-field model of relaxation dynamics of a ferrimagnet developed by Mentink *et al.* [20,33]. In this model, the longitudinal dynamics of S_A and S_B are governed by the interplay between the intersublattice exchange and spin-lattice relaxation of individual sublattices. We neglect transversal magnetization dynamics since they have experimentally been shown to be of no relevance [31], and even atomistic spin model simulations themselves have shown that transversal dynamics are only relevant at nanometer spatial scales, averaging out to zero at experimentally relevant dimensions [34]. The coupled equations of motion characterizing the temperature-dependent angular momentum of each sublattice (which are treated as a pair of macrospins) are

$$\frac{dS_A}{dt} = -\lambda_e(H_B - H_A) + \lambda_A H_A, \quad (1)$$

$$\frac{dS_B}{dt} = \lambda_e(H_B - H_A) + \lambda_B H_B, \quad (2)$$

where λ_A and λ_B characterize the flow of angular momentum from the indicated sublattice to the external environment (of temperature T), and λ_e characterizes the intersublattice exchange relaxation. The effective magnetic fields H acting on the two sublattices are derived from a microscopic Heisenberg spin Hamiltonian [33,35]. A full description of the mean-field model is supplied in Supplementary Material Note 1 [36].

Using Eqs. (1) and (2), we calculate the sublattice-resolved magnetization dynamics of $A_{100-x}B_x$ in response to thermal pulses of varying duration. Material parameters typical of the ferrimagnetic alloy $Gd_x(FeCo)_{100-x}$ are adopted [28,37,38], taking the transition metal component as a single sublattice and using concentration-independent material properties (thus restricting the independent parameters to just λ_e , λ_A , and λ_B). The full duration at half-maximum τ of the temporally Gaussian pulse enters the model through a time-dependent temperature that captures the spirit of the two-temperature model [39,40].

Figure 2 shows the results of the calculations for the alloy $Gd_{26}Fe_{74}$, obtained with varying pulse duration τ . With $\tau = 100$ fs [Fig. 2(a)], we successfully achieve deterministic AOS via different demagnetization rates and the clear formation of a transient ferromagneticlike state, whereby S_{Fe} crosses zero before S_{Gd} . Generally, increasing

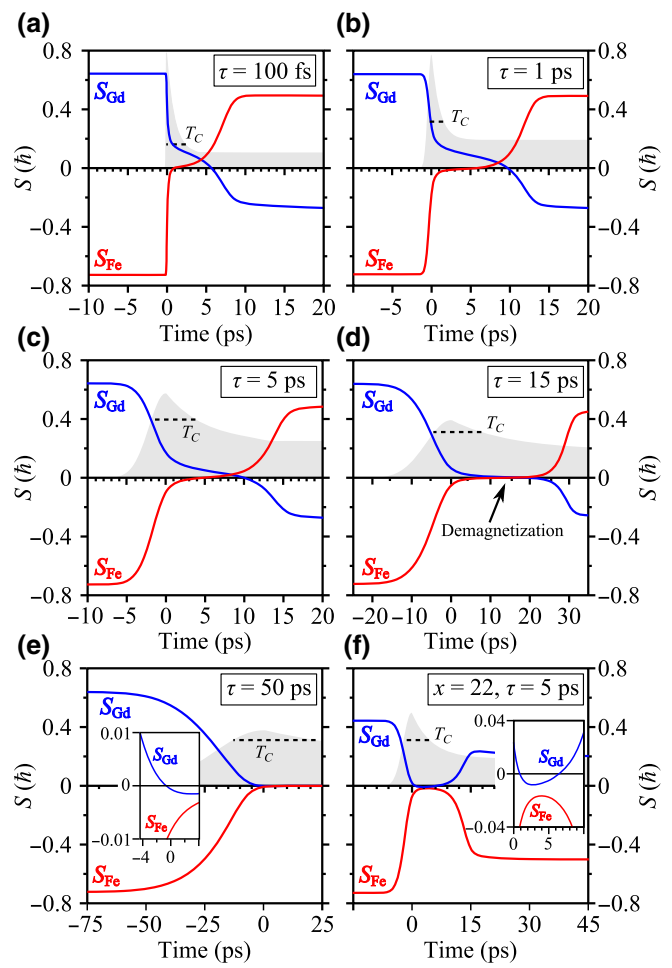


FIG. 2. (a)–(e) Calculated time-resolved traces of the angular momentum S of master sublattice Fe (red line) and slave sublattice Gd (blue line) in the ferrimagnet $Gd_{26}Fe_{74}$ for different pulse durations τ as indicated. (f) The same calculations as shown in panels (a)–(e) but for the ferrimagnet $Gd_{22}Fe_{78}$ with $\tau = 5$ ps. The grey shaded area indicates the profile of the temperature pulse (relative to a baseline of 300 K), with the dashed line indicating the corresponding equilibrium Curie temperature T_C of the ferrimagnet. Shown in the inset of panels (e) and (f) are enlarged sections.

τ leads to increasingly comparable demagnetizing rates of Gd and Fe. Stretching the pulse duration to 1 ps [Fig. 2(b)], 5 ps [Fig. 2(c)], and 15 ps [Fig. 2(d)] still enables deterministic AOS, but in the lattermost case, S_{Gd} and S_{Fe} almost completely reach zero simultaneously. In practice, thermal fluctuations would dominate at this point, and the switching would become random, losing its deterministic character. Upon stretching the pulse duration even further [Fig. 2(e)], the polarity of the transient ferromagnetic state undergoes reversal [30,41,42], i.e., the magnetization of the slave switches before that of the master. This can be explained by considering that the thermally induced demagnetization rate of each sublattice can be controlled

by tuning the initial ambient temperature T_0 of the ferrimagnet [30] with respect to the equilibrium Curie temperature T_C . Specifically, Ref. [30] shows that if $T_0/T_C < 0.6$, iron can demagnetize faster than gadolinium, but upon increasing the ratio T_0/T_C towards unity, gadolinium can demagnetize faster than iron. In the case here, the pulse duration is stretched long enough to allow slave gadolinium to demagnetize faster. In Fig. 2(f), we also show the sublattice-resolved angular momentum dynamics of the ferrimagnet $\text{Gd}_{22}\text{Fe}_{78}$ triggered by a pulse of duration 5 ps. We again clearly observe a transient ferromagneticlike state but with S_{Gd} crossing zero before S_{Fe} , again consistent with the results reported in Refs. [30,41,42]. We note that this feature is composition dependent, and becomes more pronounced in our calculations upon decreasing the concentration of slave gadolinium. We find that for all cases where this opposite polarity of the transient ferromagneticlike state is achieved, single-shot AOS is not realized.

By recasting the time-resolved trajectories of S_{Gd} and S_{Fe} as functions of each other, we acquire a numerically supported insight of how the pulse duration controls the process of deterministic AOS. Figure 3(a) shows that by increasing τ , the AOS trajectory initially becomes more linear, and then curves below the figure diagonal, reflecting the increasing dominance of the intersublattice exchange coupling. By repeating the same calculations for $\text{Gd}_x\text{Fe}_{100-x}$ alloys with varying x and fixed pulse duration $\tau = 2$ ps [Fig. 3(b)], the initial ferrimagnetic state in the plane $S_{\text{Fe}}-S_{\text{Gd}}$ is shifted upwards. This permits a steeper gradient of the AOS trajectory where S_{Fe} crosses zero while S_{Gd} is still demagnetizing. Physically, this scenario allows a ferrimagnet with more slave Gd constituents to be deterministically switched using a temporally longer pulse. Conversely, by reducing x , we find that there is a limit beyond which switching cannot occur. When $x = 22$ in Fig. 3(b), for example, the angular momentum of the slave sublattice Gd crosses zero first, and so the system returns back to its initial state, i.e., deterministic AOS is disabled.

IV. EXPERIMENTAL RESULTS

To obtain ultimate experimental evidence of our interpretation, a set of experiments is performed exposing six Gd-Fe-Co alloys with different sublattice concentrations to single laser pulses of varying duration. The samples are all of elemental composition $\text{Gd}_x(\text{FeCo})_{100-x}$, with $22 \leq x \leq 27$, and all possess out-of-plane magnetocrystalline anisotropy. Specific details of the samples are supplied [36] in Supplementary Material Note 2. The laser pulses have a photon energy of 1.55 eV (central wavelength 800 nm) and a duration that can be adjusted between 60 fs and 6.0 ps with an accuracy of <100 fs. The effect of the optical pulse on the sample magnetization is monitored

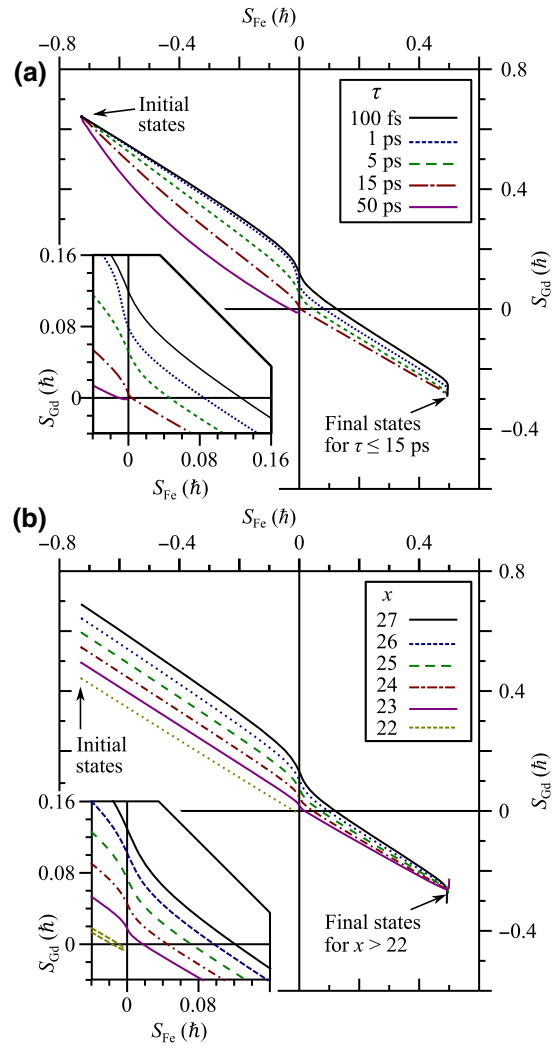


FIG. 3. (a) Phase map of the sublattice-resolved angular momentum trajectories of the ferrimagnet $\text{Gd}_{26}\text{Fe}_{74}$ obtained using different τ . Shown in the inset is an enlarged section. (b) Same as in panel (a) except $\tau = 2$ ps and the alloy concentration of the ferrimagnet $\text{Gd}_x\text{Fe}_{100-x}$ is varied.

at room temperature using a magneto-optical microscope sensitive to the out-of-plane component of magnetization via the Faraday effect.

In general, after exposure to single optical pulses of duration τ , the static images of the resulting magnetization distribution across the studied Gd-Fe-Co samples are categorized in two distinct ways. Indicative examples are provided in the insets of Fig. 4, recorded for the alloy $\text{Gd}_{23}(\text{FeCo})_{77}$. In the first case (bottom-right inset of Fig. 4), with $\tau = 1.4$ ps, deterministic AOS is observed. The pulses are either observed to toggle the magnetization spanning the entire extent of the irradiated region, or toggle only the outer perimeter of the irradiated magnetization, where the optically supplied energy is sufficiently low. In these experiments, the optical pulse is linearly polarized,

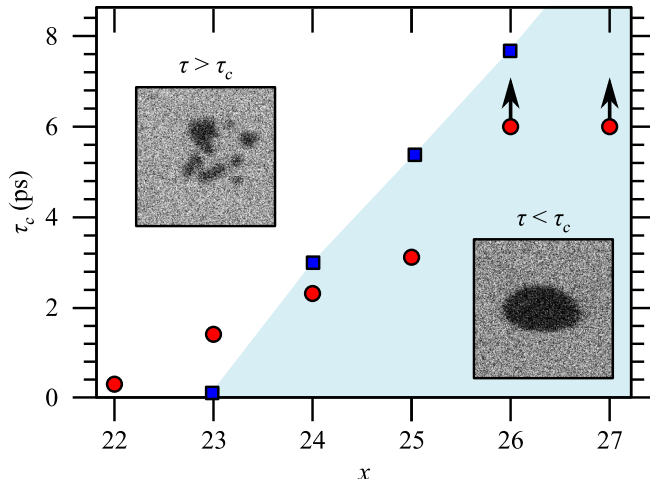


FIG. 4. The critical pulse-duration threshold τ_c is plotted (red circles) as a function of alloy composition for $\text{Gd}_x(\text{FeCo})_{100-x}$, measured using pulses of photon energy of 1.55 eV. Deterministic AOS is achieved if $\tau < \tau_c$, but disabled if $\tau > \tau_c$. Experimentally, we could only realize $\tau \leq 6$ ps, and so can only conclude that $\tau_c > 6$ ps for $x \geq 26$. Also shown are the calculated values of τ_c for the alloy $\text{Gd}_x\text{Fe}_{100-x}$ (blue squares). Insets: typical background-corrected magneto-optical images, of side length 200 μm , obtained for $\text{Gd}_{23}(\text{FeCo})_{77}$ showing deterministic AOS (bottom-right panel, $\tau = 1.4$ ps) and demagnetization (top-left inset, $\tau = 1.5$ ps). The contrast in the images is proportional to the out-of-plane component of magnetization.

and introducing circular polarization serves only to reduce or increase the fluence required [43] to achieve single-shot AOS. In the second case, with $\tau = 1.5$ ps, the optical pulse results in demagnetization only (top-left inset of Fig. 4), with a random distribution of magnetic domains forming after the arrival of each pulse. Further images showing the impact of multiple pulses are supplied [36] in Supplementary Material Note 3. Further measurements show that pulse durations below and above 1.4 ps always result in deterministic AOS and demagnetization respectively, and thus we conclude that $\text{Gd}_{23}(\text{FeCo})_{77}$ possesses a critical threshold $\tau_c = 1.4$ ps whereby deterministic AOS is enabled if $\tau < \tau_c$ but is disabled if $\tau > \tau_c$.

We repeat the measurements shown in the insets of Fig. 4 for each $\text{Gd}_x(\text{FeCo})_{100-x}$ alloy, and presented in Fig. 4 are the corresponding thresholds τ_c as a function of x . Clearly, as the percentage of the slave gadolinium in $\text{Gd}_x(\text{FeCo})_{100-x}$ increases, the pulse duration still capable of enabling deterministic AOS increases monotonically. When $x \geq 26$, we are unable to identify the threshold which exceeds 6.0 ps (a limit imposed by our regenerative amplifier). However, in Ref. [22], $\tau_c = 15$ ps for $x = 27.5$, which is in good agreement with the implications of our results. Using the calculations, we obtain a similar trend, taking in to account that thermal fluctuations disable single-shot AOS if S_{Fe} and S_{Gd} cross zero almost simultaneously. In

particular, because the thermal energy delivered by the laser pulse is Gaussian in space, our experiments allow us to distinguish the impact of the pulse duration from that of the incident fluence. If the incident fluence is excessive but the pulse duration is below τ_c , we generate demagnetization encircled by a toggled perimeter of magnetization. The demagnetization originates from S_{Fe} and S_{Gd} crossing zero almost simultaneously, but the toggled perimeter of magnetization (where the local fluence is lower) reveals single-shot AOS is achievable. If, however, no such toggled perimeter of magnetization exists, we can deduce $\tau > \tau_c$. Despite the many simplifying assumptions inherent to our numerical model (e.g., using fixed material parameters that are generally independent of x , ignoring the role of spatial inhomogeneities [41], etc.), the numerical and experimental findings are in a good agreement with our conceptual understanding [36]. Thus, we believe that one can obtain deep physical insight into the single-shot helicity-independent switching process by considering AOS trajectories across the S_A - S_B plane.

A fundamental assumption of our model lies in our use of the concept of “temperature” itself. Temperature can be associated with equilibrium phenomena only [44], but it is routinely used in descriptions of nonequilibrium magnetization dynamics [13,18,20,45]. An optical excitation of high photon energy at a value of 1.55 eV stimulates a multitude of intraband and interband electronic excitations, causing the temperature of the spins to become poorly defined [22]. The importance of these high-energy excitations in the effectiveness of the demagnetization process was also a subject of recent theoretical debate [46,47]. As efficient and fast demagnetization is an essential prerogative for switching in our model, we can provide a direct experimental answer to this problem by considerably reducing the photon energy of the optical excitation. We therefore use pulses in the midinfrared spectral range at Free Electron Lasers for Infrared eXperiments (FELIX) [48,49]. A single linearly polarized optical pulse, with photon energy ranging between $E = 70$ meV and $E = 230$ meV, is focused to a spot of diameter 100 μm [50] on the surface of the Gd-Fe-Co samples. The duration of the pulse is controlled through cavity desynchronization [36,51], allowing the latter to be varied between approximately 400 fs and at least 6.5 ps.

Using the midinfrared optical pulses, it is possible to both enable and disable the process of single-shot AOS. In addition, it is also observed that a mixture of deterministic AOS and demagnetization can be achieved, whereby subsequent pulses have different effects on the magnetization (i.e., one pulse results in single-shot AOS, but the next pulse does not). This is consistently observed at pulse durations on the border between deterministic AOS and demagnetization, and is attributed to inescapable jitter in the pulse duration. This emphasizes even further the critical role played by the pulse duration. We supply [36] indicative

examples showing these effects in Supplementary Material Note 6.

Figure 5 shows the experimentally measured state map for $\text{Gd}_x(\text{FeCo})_{100-x}$ with $x = 24$, while the state maps for $x = 25$ and $x = 26$ are provided [36] in Supplementary Material Note 7. In these maps, we summarize how the deterministic character of AOS in $\text{Gd}_x(\text{FeCo})_{100-x}$ alloys depends on the photon energy and pulse duration, obtained through analyzing magneto-optical images recorded after exposing the material to consecutive optical pulses. For all the studied compositions of $\text{Gd}_x(\text{FeCo})_{100-x}$, we generally observe that the photon energy, despite being adjusted by a factor of more than 20 (between 70 meV and 1.55 eV), always enables deterministic AOS provided the pulse duration is sufficiently low. This result validates both the microscopic picture of ultrafast demagnetization advanced by Schellekens *et al.* in Ref. [46] and the invocation of temperature in our model. Moreover, these results confirm that relatively gentle heating of the free electrons in Gd-Fe-Co [52] (importantly still on a nonadiabatic timescale) is sufficient to achieve the necessary strongly nonequilibrium state required for single-shot AOS.

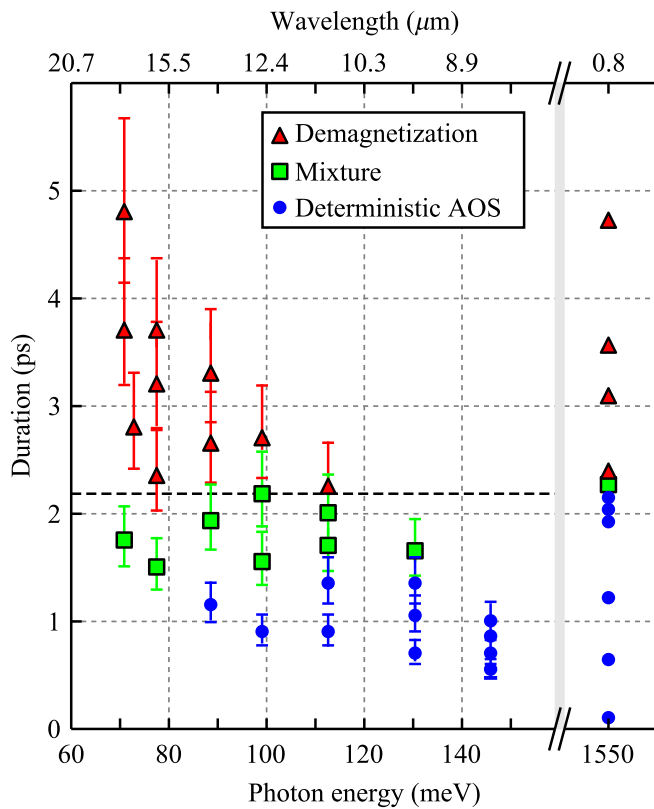


FIG. 5. State map recorded for $\text{Gd}_{24}(\text{FeCo})_{76}$ indicating how the switching process depends on the photon energy and pulse duration. Points indicated with a blue circle or red triangle correspond to observations of deterministic AOS or demagnetization respectively, whereas green squares correspond to observations of both effects arising from jitter in the pulse duration.

V. CONCLUSIONS

In summary, we present a conceptual understanding of the mechanism underpinning deterministic AOS. We base our description on there being a master-slave relationship between the constituents of a generic ferrimagnet AB , where A (the master) is ferromagnetic and B (the slave) is paramagnetic in isolation. Single-shot helicity-independent AOS can be achieved through two pathways, either by angular momentum flowing from A and B to the external bath or through angular momentum being transferred from the slave to the master. The choice of which pathway is followed depends solely on the pulse duration relative to the timescales of the spin-lattice and intersublattice exchange relaxation, and increasing the concentration of slaves in AB also increases the pulse duration that can still achieve deterministic AOS. We use a phenomenological mean-field approach to validate our understanding, and provide ultimate proof by studying how the critical pulse-duration threshold (above or below which deterministic AOS is disabled or enabled) evolves as a concentration of the slave in Gd-Fe-Co alloys. Moreover, by demonstrating that midinfrared optical pulses are capable of realizing deterministic AOS, we experimentally show that the three-temperature model offers a valid description of ultrafast magnetization dynamics, provided that suitable discrimination is made between the spin reservoirs of A and B . We believe our conceptual understanding resolves many controversies surrounding deterministic AOS, and could be deployed to understand how single-shot helicity-independent AOS can be achieved in a larger class of ferrimagnetic materials.

ACKNOWLEDGMENTS

We thank S. Semin, T. Toonen and all technical staff at FELIX for technical support. This research has received funding from the European Union's Horizon 2020 research and innovation program under FET-Open Grant Agreement No. 713481 (SPICE) and FET-Open Grant Agreement No. 737093 (FEMTOTERABYTE), de Nederlandse Organisatie voor Wetenschappelijk Onderzoek (NWO), the project TEAM/2017-4/40 of the foundation for Polish Science, and the Grant-in-Aid for Scientific Research on Innovative Area, “Nano Spin Conversion Science” (Grant No. 26103004).

- [1] I. Jakobi, P. Neumann, Y. Wang, D. B. R. Dasari, F. El Hallak, M. A. Bashir, M. Markham, A. Edmonds, D. Twitchen, and J. Wrachtrup, Measuring broadband magnetic fields on the nanoscale using a hybrid quantum register, *Nat. Nanotechnol.* **12**, 67 (2017).
- [2] J.-G. Zhu, X. Zhu, and Y. Tang, Microwave assisted magnetic recording, *IEEE Trans. Magn.* **44**, 125 (2008).

- [3] W. A. Challener, C. Peng, A. Itagi, D. Karns, W. Peng, Y. Peng, X. Yang, X. Zhu, N. J. Gokemeijer, Y.-T. Hsia, G. Ju, R. E. Rottmayer, M. A. Seigler, and E. C. Gage, Heat-assisted magnetic recording by a near-field transducer with efficient optical energy transfer, *Nat. Photonics* **3**, 220 (2009).
- [4] D. Weller, O. Mosendz, G. Parker, S. Pisana, and T. S. Santos, L₁₀ FePtX-Y media for heat-assisted magnetic recording, *Phys. Status Solidi A* **210**, 1245 (2013).
- [5] S. Xiong, R. Smith, N. Wang, D. Li, E. Schreck, S. Canchi, and Q. Dai, Thermal response time of media in heat-assisted magnetic recording, *IEEE Trans. Magn.* **53**, 3301906 (2017).
- [6] S. Okamoto, N. Kikuchi, M. Furuta, O. Kitakami, and T. Schimatsu, Microwave assisted magnetic recording technologies and related physics, *J. Phys. D: Appl. Phys.* **48**, 353001 (2015).
- [7] E. Beaurepaire, J.-C. Merle, A. Daunois, and J.-Y. Bigot, Ultrafast Spin Dynamics in Ferromagnetic Nickel, *Phys. Rev. Lett.* **76**, 4250 (1996).
- [8] A. Kirilyuk, A. V. Kimel, and Th. Rasing, Ultrafast optical manipulation of magnetic order, *Rev. Mod. Phys.* **82**, 2731 (2010).
- [9] A. Eschenlohr and U. Bovensiepen, Special issue on ultrafast magnetism, *J. Phys.: Condens. Matter* **30**, 030301 (2018).
- [10] C. D. Stanciu, F. Hansteen, A. V. Kimel, A. Kirilyuk, A. Tsukamoto, A. Itoh, and Th. Rasing, All-Optical Magnetic Recording with Circularly Polarized Light, *Phys. Rev. Lett.* **99**, 047601 (2007).
- [11] K. Vahaplar, A. M. Kalashnikova, A. V. Kimel, S. Gerlach, D. Hinzke, U. Nowak, R. Chantrell, A. Tsukamoto, A. Itoh, A. Kirilyuk, and Th. Rasing, All-optical magnetization reversal by circularly polarized laser pulses: Experiment and multiscale modeling, *Phys. Rev. B* **85**, 104402 (2012).
- [12] U. Atxitia and T. A. Ostler, Ultrafast double magnetization switching in GdFeCo with two picosecond-delayed femtosecond pump pulses, *Appl. Phys. Lett.* **113**, 062402 (2018).
- [13] T. A. Ostler, et al., Ultrafast heating as a sufficient stimulus for magnetization reversal in a ferrimagnet, *Nat. Commun.* **3**, 666 (2012).
- [14] C.-H. Lambert, S. Mangin, B. S. D. Ch, S. Varaprasad, Y. K. Takahashi, M. Hehn, M. Cinchetti, G. Malinowski, K. Hono, Y. Fainman, M. Aeschlimann, and E. E. Fullerton, All-optical control of ferromagnetic thin films and nanostructures, *Science* **345**, 1337 (2014).
- [15] S. Mangin, M. Gottwald, C.-H. Lambert, D. Steil, V. Uhlíř, L. Pang, M. Hehn, S. Alebrand, M. Cinchetti, G. Malinowski, Y. Fainman, M. Aeschlimann, and E. E. Fullerton, Engineered materials for all-optical helicity-dependent magnetic switching, *Nat. Mater.* **13**, 286 (2014).
- [16] M. L. M. Lalieu, M. J. G. Peeters, S. R. R. Haenen, R. Lavrijsen, and B. Koopmans, Deterministic all-optical switching of synthetic ferrimagnets using single femtosecond laser pulses, *Phys. Rev. B* **96**, 220411(R) (2017).
- [17] L. Avilés-Félix, L. Álvaro-Gómez, G. Li, C. S. Davies, A. Olivier, M. Rubio-Roy, S. Auffret, A. Kirilyuk, A. V. Kimel, Th. Rasing, L. D. Buda-Prejbeanu, R. C. Sousa, B. Dieny, and I. L. Prejbeanu, Integration of Tb/Co multilayers within optically switchable perpendicular magnetic tunnel junctions, *AIP Adv.* **9**, 125328 (2019).
- [18] I. Radu, K. Vahaplar, C. Stamm, T. Kachel, N. Pontius, H. A. Dürr, T. A. Ostler, J. Barker, R. F. L. Evans, R. W. Chantrell, A. Tsukamoto, A. Itoh, A. Kirilyuk, Th. Rasing, and A. V. Kimel, Transient ferromagnetic-like state mediating ultrafast reversal of antiferromagnetically coupled spins, *Nature* **472**, 205 (2011).
- [19] I. Radu, et al., Ultrafast and distinct spin dynamics in magnetic alloys, *Spin* **5**, 1550004 (2015).
- [20] J. H. Mentink, J. Hellsvik, D. V. Afanasiev, B. A. Ivanov, A. Kirilyuk, A. V. Kimel, O. Eriksson, M. I. Katsnelson, and Th. Rasing, Ultrafast Spin Dynamics in Multisublattice Magnets, *Phys. Rev. Lett.* **108**, 057202 (2012).
- [21] D. Steil, S. Alebrand, A. Hassdenteufel, M. Cinchetti, and M. Aeschlimann, All-optical magnetization recording by tailoring optical excitation parameters, *Phys. Rev. B* **84**, 224408 (2011).
- [22] J. Gorchon, R. B. Wilson, Y. Yang, A. Pattabi, J. Y. Chen, L. He, J. P. Wang, M. Li, and J. Bokor, Role of electron and phonon temperatures in the helicity-independent all-optical switching of GdFeCo, *Phys. Rev. B* **94**, 184406 (2016).
- [23] O. Eriksson, A. Bergman, L. Bergqvist, and J. Hellsvik, *Atomistic Spin Dynamics: Foundations and Applications* (Oxford University Press, New York, 2017).
- [24] E. Iacocca, et al., Spin-current-mediated rapid magnon localisation and coalescence after ultrafast optical pumping of ferrimagnetic alloys, *Nat. Commun.* **10**, 1756 (2019).
- [25] K. Vahaplar, A. M. Kalashnikova, A. V. Kimel, D. Hinzke, U. Nowak, R. Chantrell, A. Tsukamoto, A. Itoh, A. Kirilyuk, and Th. Rasing, Ultrafast Path for Optical Magnetization Reversal via a Strongly Nonequilibrium State, *Phys. Rev. Lett.* **103**, 117201 (2009).
- [26] L. Chusseau and C. Kazmierski, Optimum linear pulse compression of a gain-switched 1.5 μm DFB laser, *IEEE Photonics Tech. Lett.* **6**, 24 (1994).
- [27] M. Beens, M. L. M. Lalieu, A. J. M. Deenen, R. A. Duine, and B. Koopmans, Comparing all-optical switching in synthetic-ferrimagnetic multilayers and alloys, *Phys. Rev. B* **100**, 220409(R) (2019).
- [28] T. A. Ostler, R. F. L. Evans, R. W. Chantrell, U. Atxitia, O. Chubykalo-Fesenko, I. Radu, R. Abrudan, F. Radu, A. Tsukamoto, A. Itoh, A. Kirilyuk, Th. Rasing, and A. Kimel, Crystallographically amorphous ferrimagnetic alloys: Comparing a localized atomistic spin model with experiments, *Phys. Rev. B* **84**, 024407 (2011).
- [29] A. Melnikov, H. Prima-Garcia, M. Lisowski, T. Gießel, R. Weber, R. Schmidt, C. Gahl, N. M. Bulgakova, U. Bovensiepen, and M. Weinelt, Nonequilibrium Magnetization Dynamics of Gadolinium Studied by Magnetic Linear Dichroism in Time-Resolved 4f Core-Level Photoemission, *Phys. Rev. Lett.* **100**, 107202 (2008).
- [30] U. Atxitia, J. Barker, R. W. Chantrell, and O. Chubykalo-Fesenko, Controlling the polarity of the transient ferromagneticlike state in ferrimagnets, *Phys. Rev. B* **89**, 224421 (2014).

- [31] Y. Tsema, Doctoral Thesis, Radboud University Nijmegen, 2017.
- [32] B. Koopmans, G. Malinowski, F. Dalla Longa, D. Steiauf, M. Fähnle, T. Roth, M. Cinchetti, and M. Aeschlimann, Explaining the paradoxical diversity of ultrafast laser-induced demagnetization, *Nat. Mater.* **9**, 259 (2010).
- [33] J. H. Mentink, Doctoral Thesis, Radboud University Nijmegen, 2012.
- [34] U. Atxitia, T. Ostler, J. Barker, R. F. L. Evans, R. W. Chantrell, and O. Chubykalo-Fesenko, Ultrafast dynamical path for the switching of a ferrimagnet after femtosecond heating, *Phys. Rev. B* **87**, 224417 (2013).
- [35] R. Jedynak, New facts concerning the approximation of the inverse Langevin function, *J. Non-Newton Fluid.* **249**, 8 (2017).
- [36] See Supplementary Material at <http://link.aps.org-supplemental/10.1103/PhysRevApplied.13.024064> for a brief discussion of the modeling methodology, the full composition of the samples studied, and further experimental and numerical results supporting our conclusions.
- [37] Y. Mimura, N. Imamura, T. Kobayashi, A. Okada, and Y. Kushiro, Magnetic properties of amorphous alloy films of Fe with Gd, Tb, Dy, Ho, or Er, *J. Appl. Phys.* **49**, 1208 (1978).
- [38] P. Hansen, S. Klahn, C. Clausen, G. Much, and K. Witter, Magnetic and magneto-optical properties of rare-earth transition-metal alloys containing Dy, Ho, Fe, Co, *J. Appl. Phys.* **69**, 3194 (1991).
- [39] U. Atxitia, T. A. Ostler, R. W. Chantrell, and O. Chubykalo-Fesenko, Optimal electron, phonon, and magnetic characteristics for low energy thermally induced magnetization switching, *Appl. Phys. Lett.* **107**, 192402 (2015).
- [40] J. Kimling, J. Kimling, R. B. Wilson, B. Hebler, M. Albrecht, and D. G. Cahill, Ultrafast demagnetization of FePt: Cu thin films and the role of magnetic heat capacity, *Phys. Rev. B* **90**, 224408 (2014).
- [41] C. E. Graves, et al., Nanoscale spin reversal by non-local angular momentum transfer following ultrafast laser excitation in ferrimagnetic GdFeCo, *Nat. Mater.* **12**, 293 (2013).
- [42] R. Chimata, L. Isaeva, K. Kádas, A. Bergman, B. Sanyal, J. H. Mentink, M. I. Katsnelson, Th. Rasing, A. Kirilyuk, A. Kimel, O. Eriksson, and M. Pereiro, All-thermal switching of amorphous Gd-Fe alloys: Analysis of structural properties and magnetization dynamics, *Phys. Rev. B* **92**, 094411 (2015).
- [43] A. R. Khorsand, M. Savoini, A. Kirilyuk, A. V. Kimel, A. Tsukamoto, A. Itoh, and Th. Rasing, Role of Magnetic Circular Dichroism in All-Optical Magnetic Recording, *Phys. Rev. Lett.* **108**, 127205 (2012).
- [44] A. Puglisi, A. Sarracino, and A. Vulpiani, Temperature in and out of equilibrium: A review of concepts, tools and attempts, *Phys. Rep.* **709**, 1 (2017).
- [45] S. Wienholdt, D. Hinzke, K. Carva, P. M. Oppeneer, and U. Nowak, Orbital-resolved spin model for thermal magnetization switching in rare-earth-based ferrimagnets, *Phys. Rev. B* **88**, 020406(R) (2013).
- [46] A. J. Schellekens and B. Koopmans, Comparing Ultrafast Demagnetization Rates Between Competing Models for Finite Temperature Magnetism, *Phys. Rev. Lett.* **110**, 217204 (2013).
- [47] W. Töws and G. M. Pastor, Many-Body Theory of Ultrafast Demagnetization and Angular Momentum Transfer in Ferromagnetic Transition Metals, *Phys. Rev. Lett.* **115**, 217204 (2015).
- [48] D. Oepts, A. F. G. van der Meer, and P. W. van Amersfoort, The free-electron-laser user facility FELIX, *Infrared Phys. Technol.* **36**, 297 (1995).
- [49] G. M. H. Knippels and A. F. G. van der Meer, FEL diagnostics and user control, *Nucl. Instrum. Methods Phys. Res.* **144**, 32 (1998).
- [50] J. M. Liu, Simple technique for measurements of pulsed Gaussian-beam spot sizes, *Opt. Lett.* **7**, 196 (1982).
- [51] R. J. Bakker, D. A. Jaroszynski, A. F. G. van der Meer, D. Oepts, and P. W. van Amersfoort, Short-pulse effects in a free-electron laser, *IEEE J. Quantum Electron.* **30**, 1635 (1994).
- [52] Y. Yang, R. B. Wilson, J. Gorchon, C.-H. Lambert, S. Salahuddin, and J. Bokor, Ultrafast magnetization reversal by picosecond electrical pulses, *Sci. Adv.* **3**, 1603117 (2017).